STAGING OF TWO-STAGE-TO-ORBIT AEROSPACE PLANE

Kenji Kudo,* and Takeshi Kanda*
***Japan Aerospace Exploration Agency, Space Propulsion Research Center**
Kakuda, Miyagi, Japan 981-1525

Keywords: *Aerospace plane, Staging, Unstart, Trajectory, Pitching moment*

Abstract

At the staging of the Two-Stage-to-Orbit aerospace plane, the engine will be in the shutdown condition and the intake will be in the unstarted condition. The effect of the drag due to the unstarted engine on the flight trajectory was investigated. Next the effect of the engine operating condition on the pitching moment of the first stage vehicle was discussed. The net drag increased with the unstarted intake, and the horizontal distance between the vehicles became larger. The change of the engine operating condition by shutdown affected the pitching moment of the first stage vehicle. The unstarted intake did not affect the pitching moment greatly.

Nomenclature

C_D = drag coefficient
C_L = lift coefficient
c_m = mean chord length
D = drag
F = force
g = acceleration of gravity at height of z
I_{sp} = specific impulse
L = lift (Fig. 3), length of airframe (Fig. 4)
M = Mach number
m = mass
P = pressure
R = radius of the Earth
S = surface area of wing
v = velocity
y_{CG} = vertical distance from bottom of airframe to center of gravity of 1st stage vehicle
x = distance on the Earth surface (Fig. 3), horizontal distance from leading edge of airframe (Fig. 4)
x_{CG} = horizontal distance from leading edge of airframe to center of gravity of 1st stage vehicle
z = height of the aerospace plane from surface of the Earth
α = angle of attack
δ = angle between engine thrust and airframe velocity
γ = angle of inclination
1 = first stage vehicle, No.1 area (Fig. 2)
2 = second stage vehicle, No.2 area (Fig. 2)
3,4,5 = No. 3, 4, 5 area (Fig. 2)

1 Introduction

Aerospace planes with the air-breathing engine have been studied. Most of the planes belong to the Single-Stage-to-Orbit (SSTO) aerospace plane or the Two-Stage-to-Orbit (TSTO) aerospace plane. Figure 1 shows a conceptual image of the TSTO plane.[1] Some of the TSTO plane systems adopt the Air-Turbo-Ramjet (ATR) engine for take-off and acceleration of the first stage. Staging Mach number is around 4.5. When the ATR uses an inter-cooler to cool down the inflow air, the staging Mach number is around 6. Some of the plane systems adopt the scramjet. Then, the staging Mach number is around 10 to 12. The second stage vehicle usually adopts the liquid

Fig. 1. Image of TSTO plane.

rocket engine. Studies on the TSTO plane, e.g., the aerodynamic interaction between the first stage and the second stage vehicles[2,3] and the conceptual design of vehicles and flight trajectory[4-10] have been conducted.

At staging, the first stage vehicle releases the second stage vehicle, and the mass of the vehicle becomes approximately half due to disconnection of the second stage vehicle. The gravity force acting to the first stage vehicle decreases. On the other hand, the lift to the first stage is the same as that before staging, which is almost sufficient to support the two vehicles. Therefore, upward force acts to the first stage vehicle after staging, and the first stage vehicle goes upward. On the second stage vehicle, lift is small and mass is large due to no propellant consumption at the staging. Therefore, the second stage vehicle flies up gradually. The two vehicles hardly separate and might collide just after staging. Therefore, the staging schedule of the TSTO plane is as follows.[10]

Before staging, the first stage vehicle flies with little angle of attack, i.e., under little lift condition, and under shutting down the engine not to scrub the orbital stage vehicle and not to damage the vehicle with the exhaust gas after releasing. Then the first stage releases the second stage vehicle. The second stage vehicle has several angles of attack, pitch-ups and goes apart from the first stage vehicle. When the vehicles are apart sufficiently, the second stage vehicle starts to operate the rocket engine.

Prior to the staging, the TSTO vehicle flies

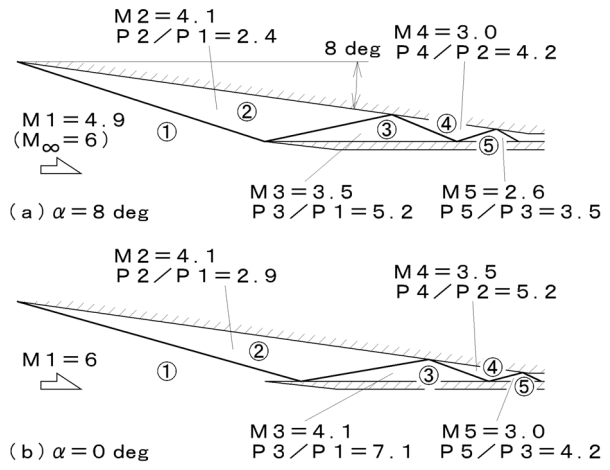

Fig. 2. Comparison of shock waves in intake.

with an angle of attack of around 8 deg.[11] When the engine is attached on the windward surface of the first stage vehicle, air pre-compressed by the airframe forebody enters the ATR or the scramjet. When the engines are on the wing, the engines are inclined for air to come straight to the engine. At staging, the angle of attack is around 0, and air is not pre-compressed by the forebody or comes to the engine at an angle of attack with several degrees. The shock waves in the intake are out of the design condition, and the intake will be in the unstarted condition. Figure 2 shows the shock waves in the intake under the 8-deg angle of attack condition and the no angle of attack condition, calculated with the 2-D shock wave relations. In the design condition, the ramp shock impinges on the leading edge of the cowl. In the no angle condition, the ramp shock impinges on the surface of the cowl, and the pressure ratio becomes larger. This higher pressure will induce separation of airflow. Then inflow supersonic air cannot be ingested by the intake sufficiently and overflow the intake; the intake is in the unstarted condition.

On the leeward surface of inclined wing or body of revolution, separation of airflow may be induced.[12-13] At the staging under the condition with little angle of attack, the aerospace plane shows the configuration with the space-side surface as ‘windward’ surface and the ground-side as ‘leeward’ surface. Pressure on the ground-side surface becomes lower than pressure on the space-side. The pressure difference may induce the secondary flow on the ground-side surface. Separation may be induced on the ‘leeward’ ground-side surface on which the engines are mounted.[14] The intake ingests the separated air and will become unstarted. Even when the separation is not induced, the boundary layer on the ground-side surface becomes thicker due to decreased Reynolds number under the condition with no angle of attack.[15] This thick boundary layer will induces the unstarted condition of the intake.

Under the unstarted condition of the intake, drag of the engine increases, comparing with that under the started condition of the intake. In the engine-shutdown condition, especially, in

the unstarted condition of the intake, contribution of the engine to the pitching moment of the first stage vehicle becomes opposite direction to the direction during the operation of the engine. In the paper, first, the effect of the unstarted condition on the flight trajectory of the first stage vehicle is discussed. Then the effect of the engine operating condition on the pitching moment of the first stage vehicle is discussed.

2 Calculation Procedures

2.1 Flight Simulation of Aerospace Plane

The simulation methods of the flight of the plane were the same as those used in a previous investigation.[11]

$$\frac{dx}{dt} = \frac{R}{R+z} \cdot v \cdot \cos\gamma \tag{1}$$

$$\frac{dz}{dt} = v \cdot \sin\gamma \tag{2}$$

$$\frac{dv}{dt} = \frac{F \cdot \cos\delta - D}{m} - g \cdot \sin\gamma \tag{3}$$

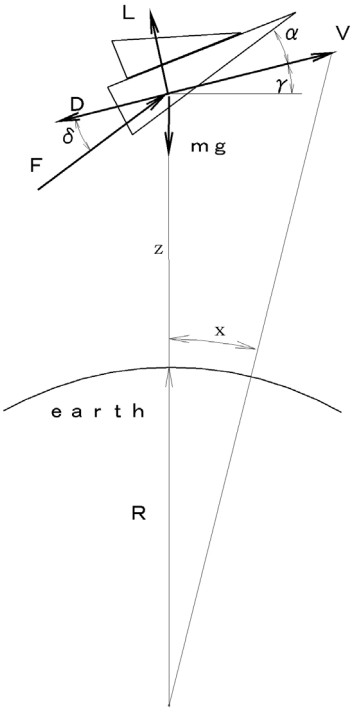

Fig. 3. Forces, velocity, and coordinates on aerospace plane.

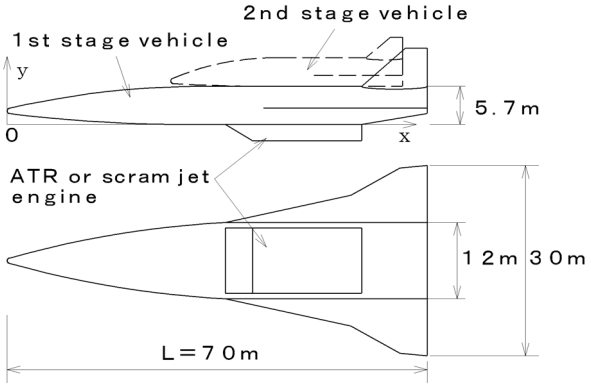

Fig. 4. Schematic diagram of TSTO plane.

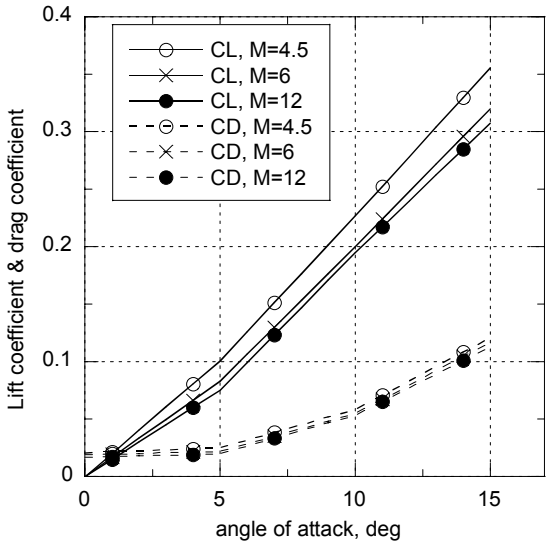

Fig. 5. Lift coefficient and drag coefficient of airframe.

$$\frac{d\gamma}{dt} = \frac{F \cdot \sin\delta + L}{m \cdot v} - \frac{g \cdot \cos\gamma}{v} + \frac{v \cdot \cos\gamma}{R+z} \tag{4}$$

$$\frac{dm}{dt} = -\frac{F}{I_{sp}} \tag{5}$$

The first stage and the second stage vehicles were treated as material points. They were at the same position at start of staging. The flight path was on a two-dimensional plane. The simulation was conducted from the release of the second stage at three staging Mach numbers of 4.5, 6 and 12 under the flight dynamic pressure of 50 kPa. As described in the introduction, they are representative conditions for the TSTO planes. The schematic diagram of the forces is shown in Fig. 3.

Figure 4 shows the airframe configuration of the vehicle. The wing area, S_w, was 315 m^2.

The length of the first stage vehicle, L, was 70 m. The airframe model was originally designed for the Single-Stage-to-Orbit plane, so it had wide base area. Lift coefficient and drag coefficient of the first stage vehicle were based on the experimental data.[16] Lift was controlled with the angle of attack. The maximum angle of attack was 15 deg here. The lift was a function of the angle of attack and was 0 at the angle of 0 deg here. Figure 5 shows the lift and drag coefficients of the plane. The aerodynamic performances of the second stage vehicle were the same as those of the first stage here.

2.2 Airframe and Engine Conditions

The wing area of the second stage vehicle is smaller than that of the first stage. The wing area of the second stage vehicle was half of the area of the first stage. At the staging, mass of each stage vehicle was 150 Mg, assuming the total mass 350 Mg to 450 Mg of the TSTO system at take-off.[8,11]

The cross section of the ATR was 15 m^2, where as that of the scramjet was 30 m^2. Each engine was assumed to have variable geometry due to wide operating range of each engine. The minimum contraction area ratio of the intake was set to be five.

In the model of the unstarted condition of the intake, the engine configurations were simplified. The complicated flow pass in the ATR was omitted and the pass was a simple convergent-divergent duct here. The pass of the scramjet was also a simple duct. At the staging Mach number under no angle of attack, the ramp shock wave impinged on the leading edge of the cowl. In the actual intake, start ability of the intake will be improved by, e.g., a drooped cowl[17] or bleeding.

In the unstarted condition, the normal shock stood ahead of the intake cowl downstream of the ramp shock wave, and the air choked at the throat. Figure 6 shows the schematic diagram of the unstarted condition model. The contraction ratios were five in all the engines at the staging. This small ratio suppressed the drag of the intake under the unstarted condition. When the ratio is larger or

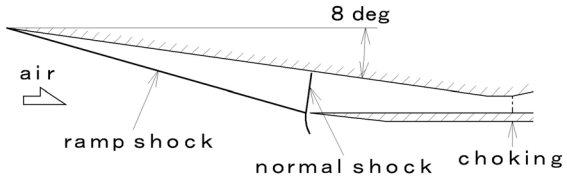

Fig. 6. Unstarted condition model of intake.

when the unstarted condition is caused by the machines inside the ATR, the drag will be increased. The mass capture ratios were 0.5 at Mach 4.5, and 0.6 at Mach 6, respectively. If the intake is kept under the started condition, the excess air has to be bled. Under the Mach 12 condition, separation of airflow due to the high pressure-ratio should be suppressed in the intake. The drag coefficients under the unstarted condition were 0.96 at Mach 4.5, 0.84 at Mach 6, and 0.44 at Mach 12, respectively. They are normalized with flight dynamic pressure and the projected cross section of the intake.

2.2 Pitching Moment

Pitching moment was positive when it was in the head-up direction. The moment arm was 0.5 m from the ground-side surface of the airframe with the ATR engine, and it was 1 m with the scramjet engine. They are approximately half of the engine height. The pressure distribution around the first stage vehicle was calculated with the newtonian flow model. The vertical position of the center of gravity of the first stage vehicle was on the bottom of the airframe, $y_{CG} = 0$, at the staging. The reference horizontal position of the center was at $x_{CG}/L = 0.5$.

In the reference condition, the second stage was mounted so that the pitching moment by the second stage was balanced at the staging around the center of gravity of the first stage vehicle. The horizontal position of the second stage mount was near the center of gravity of the first stage.

3 Results and Discussion

3.1 Effect of Unstarted Intake on Flight

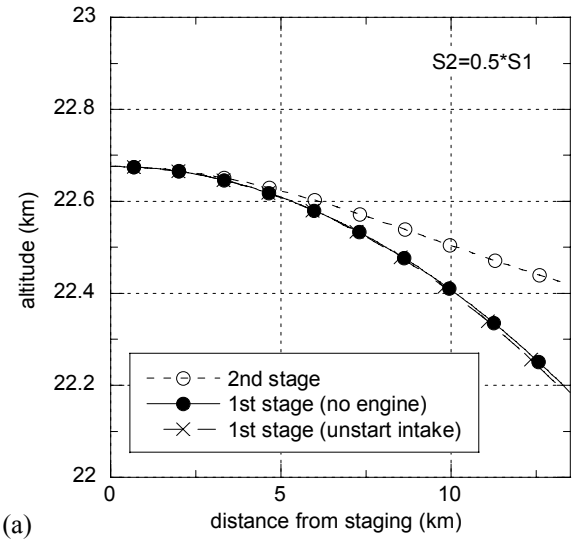

(a)

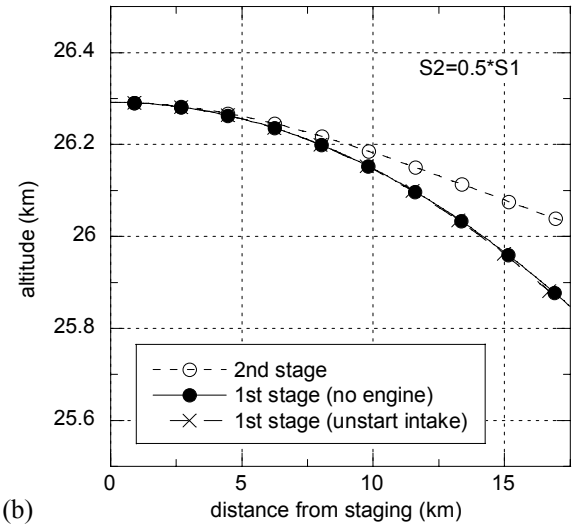

(b)

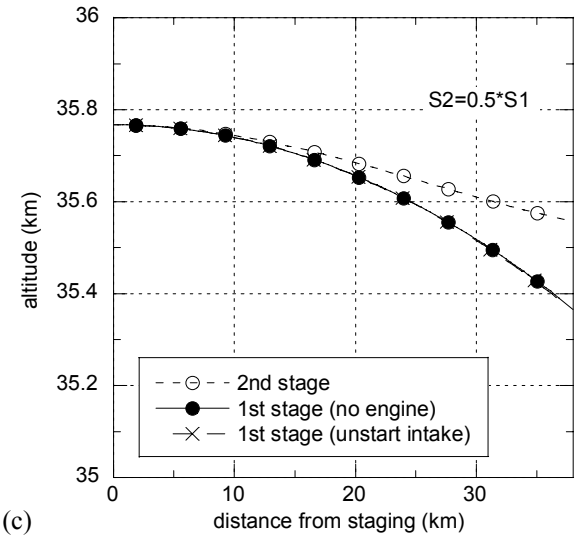

(c)

Fig.7. Flight trajectories of the first stage and the second stage vehicles. Staging Mach numbers are 4.5 in (a), 6 in (b) and 12 in (c), respectively.

Figures 7 (a) to (c) show flight trajectories of the vehicles from the release of the second stage vehicle. The inclination angle was 0 deg at the start of the staging. The first symbols are plotted at 0.5 second and the subsequent ones are every 1 second. In the simulation of the no engine condition, drag due to the engine was not included. Figure 8 shows the history of the controlled angle of attack of the second stage vehicle. When the wing area of the second stage was the same as that of the first stage, the second stage vehicle flew apart from the first stage vehicle more quickly.

The drag acting to the airframe of the first stage was larger under the unstarted-intake condition. Figure 9 shows decelerations of the first stage vehicle at the staging. When the intake was in the unstarted condition, the deceleration became more than twice. However, velocity of the vehicles was large, and the difference of trajectories between the two conditions was only several hundred meters even after ten seconds. Therefore, the effect of the unstarted intake condition was not clear in Figs. 7 (a) to (c).

Figures 10 (a) to (c) show the horizontal and vertical distances between the first stage and the second stage vehicles. They are from the second stage vehicle to the first stage, and the first stage vehicle was below and behind the second stage vehicle.

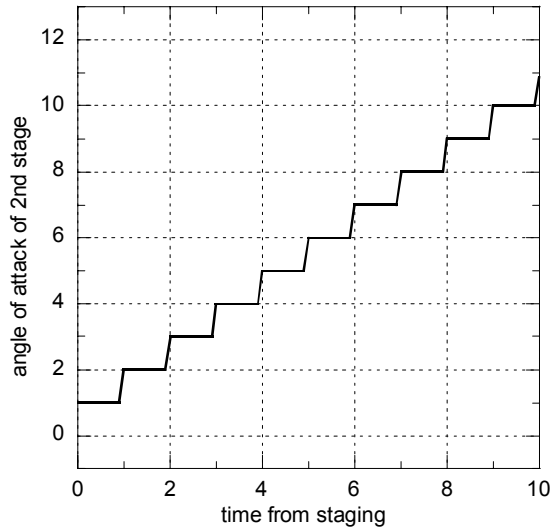

Fig. 8. History of angle of attack of the second stage vehicle.

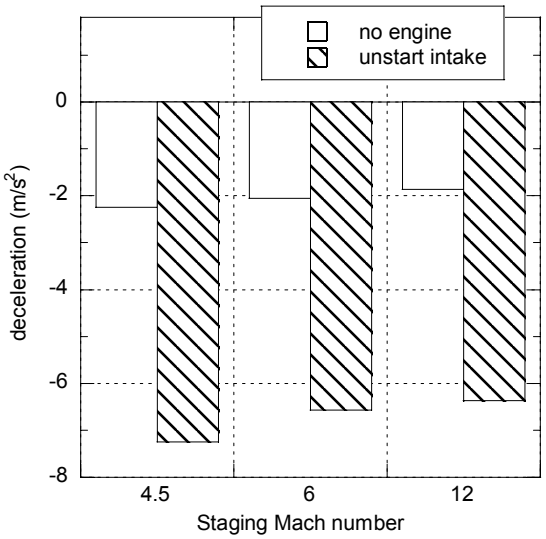

Fig. 9. Deceleration of the first stage vehicle at staging.

The vertical distances were about 200 m at 10 seconds in all the cases, and there was little difference in the vertical distances due to the unstarted condition of the intake. However, under the unstarted condition of the intake, the horizontal distance was 250 m to 300 m at 10 seconds, whereas it was about 30 m to 40 m under the no effect of the engine. These distances and differences were the in the same order of magnitude of the airframe length. The unstated condition of the intake affected the trajectory of the first stage vehicle.

3.2 Effects of Engine Operating Condition on Pitching Moment

The pitching moment was presumed to be balanced under the engine operating condition prior to staging. Figure 11 shows the change of the pitching moments of the first stage due to the engine operating condition. The moments are normalized with the wing area, the flight dynamic pressure and the one fourth of the mean chord length. The chord length was 17.5 m here. The engine thrusts were 4340 kN at Mach 4,[18] 2880 kN at Mach 6[18] and 890 kN at Mach 12, [19] respectively.

The contribution of the engine to the pitching moment was positive under the engine in operation, i.e., when the engine produced thrust. After shutdown of the engine, the

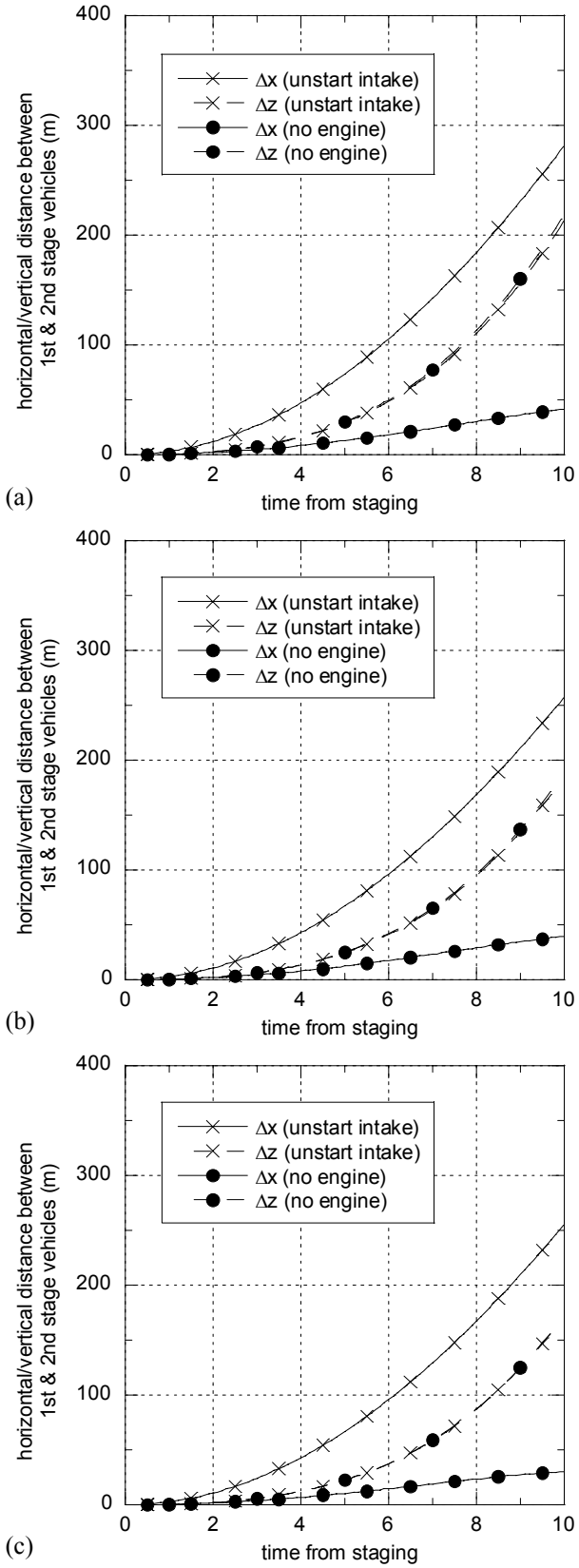

Fig.10. Horizontal/vertical distance between the first and the second stage vehicles. Staging Mach numbers are 4.5 in (a), 6 in (b) and 12 in (c), respectively.

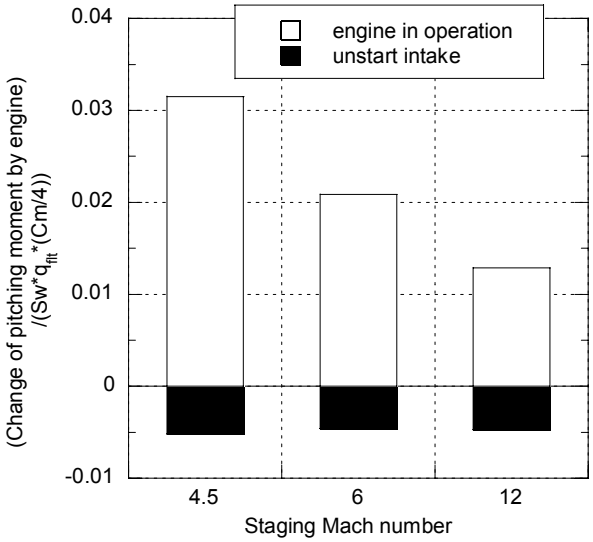

Fig. 11. Change of pitching moment due to engine operating condition.

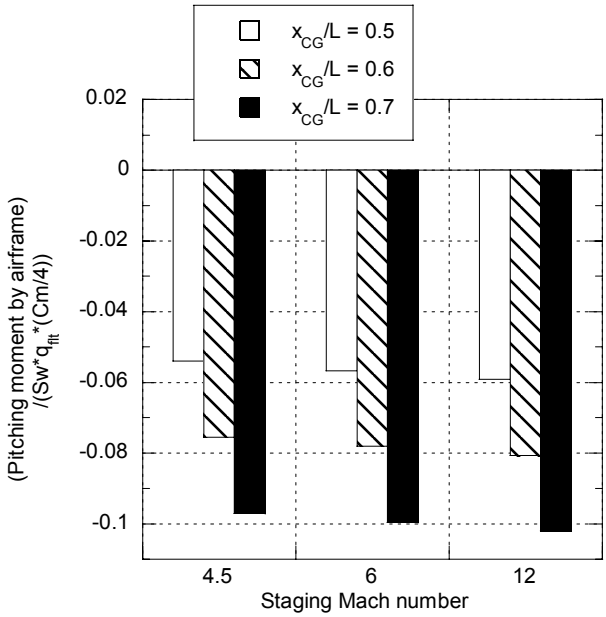

Fig. 12. Pitching moment by airframe.

contribution became negative, and it further increased due to the unstarted condition of the intake. The contribution of the engine operating condition was larger in lower staging Mach number. It was caused by larger thrust of the engine in lower Mach number. The effect of the engine operating condition on the pitching moment was primarily due to the shutdown. The effect of the drag of the unstarted engine was small.

Figure 12 shows the contribution of the first stage airframe to the pitching moment. Here the position of the center of gravity of the first stage was a parameter. One fourth of the mean chord length is also used as the reference length. The contribution did not change greatly due to the staging Mach number, because the flight dynamic pressure was the same in all the cases. As the center of gravity was downstream, the negative pitching moment on the space-side surface of the forebody became larger and the contribution became larger.

At lower staging Mach number, the contribution to the moment by the engine was in the same order of magnitude by the airframe. Therefore, the first stage vehicle should have sufficient trim ability for change of the engine operating condition during the staging.

Then the second stage was released. The pitching moment around the center of gravity of the first stage vehicle should be balanced at the staging. Figure 13 shows the change of the pitching moment around the center of the first stage by the release of the second stage. The second stage vehicle was mounted 5% length of the airframe of the first stage downstream of the center of gravity of the first stage, i.e., $x = x_{CG} + 0.05L$. Though the moment arm was long, the contribution of the aerodynamic force of the second stage vehicle to the pitching moment around the center of gravity of the first stage was small. The aerodynamic drag of the second

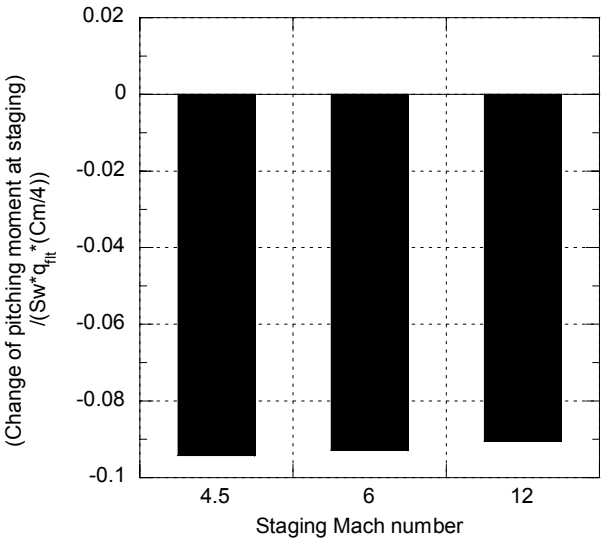

Fig. 13 Change of pitching moment at staging. Second stage vehicle was mounted 5% of airframe length downstream of the center of gravity of the first stage

stage vehicle was small due to small angle of attack. Most of the contribution was caused by the gravity force of the second stage vehicle mass. If the mount position of the second stage vehicle is not appropriate, large negative pitching moment will be produced at the release of the second stage vehicle around the center of gravity of the first stage vehicle.

4 Conclusions

Staging of the TSTO aerospace plane was investigated with the engine operating condition. The followings were made clear through the present study.

(1) When the intake of the engine was in the unstarted condition, the horizontal distance between the first stage and the second stage vehicles was larger. The unstarted condition of the intake affected the trajectory of the first stage vehicle.

(2) The effect of the engine operating condition on the pitching moment of the first stage vehicle was the similar order of magnitude of the airframe in the low staging Mach number. The largest contribution to the moment change was caused by shutdown of the engine.

Acknowledgement

The authors thank Mr. Hideyuki Taguchi, Senior Researcher of Japan Aerospace Exploration Agency, for discussion.

References

[1] http://spaceinfo.jaxa.jp/note/rocket/e/roc0012_spaceplane_e.html.

[2] Cvrlje, T., Unsteady Separation of a Two-Stage Hypersonic Vehicle, *30th AIAA Fluid Dynamic Conference*, Norfolk, VA, USA, AIAA 99-3412, 1999.

[3] Breitsamter, C., Laschka, B., Zähringer, C., and Sachs, G., Wind Tunnel Tests for Separation Dynamics Modeling of a Two-Stage Hypersonic Vehicle, *10th International Space Planes and Hypersonic Systems and Technologies Conference*, Kyoto, Japan, AIAA 2001-1811, 2001.

[4] Shirouzu, M., Mass Estimation and Sensitivity Analysis of Aerospace Plane (Part 2) 1st Report of TSTO, *Technical Memorandum of National Aerospace Laboratory*, NAL TM-602, 1989 (in Japanese).

[5] Lockwood, M. K., Hunt, J. L., Kabis, H., Moses, P., Pao, J.-L., Yarrington, P., and Collier, C., Design and Analysis of a Two-Stage-to-Orbit Airbreathing Hypersonic Vehicle Concept, *32bd Joint Propulsion Concerence*, Lake Buena Vista, FL, USA, AIAA 96-2890, 1996.

[6] Mehta, U. B., and Bowles, J. V., Two-Stage-to-Orbit Spaceplane Concept with Growth Potential, *Journal of Propulsion and Power*, Vol. 17, No. 6, pp. 1149-1161, 2001.

[7] Grallert, H., Synthesis of a FESTIP Airbreathing TSTO Space Transportation System, *Journal of Propulsion and Power*, Vol. 17, No. 6, pp. 1191-1198, 2001.

[8] Taguchi, H., Futamura, H., Yanagi, R., and Maita, M., Analytical Study pf Pre-Cooled Turbojet Engine for TSTO Spaceplane, *10th International Space Planes and Hypersonic Systems and Technologies Conference*, Kyoto, Japan, AIAA 2001-1838, 2001.

[9] Tsuchiya, T. Mori, T., and Maita, M., An Integrated Optimization for Conceptual Design of Airbreathing Launch TSTO Vehicle, *10th International Space Planes and Hypersonic Systems and Technologies Conference*, Kyoto, Japan, AIAA 2001-1902, 2001.

[10] Zähringer, C., Heller, M., and Sachs, G., Lateral Separation Dynamics and Stability of a Two-Stage Hypersonic Vehicle, *12th International Space Planes and Hypersonic Systems and Technologies Conference*, Norfolk, VA, USA, AIAA 2003-7080, 2003.

[11] Kanda, T., and Kudo, K., Payload to Low Earth Orbit by Aerospace Plane with Scramjet Engine, *Journal of Propulsion and Power*, Vol. 13, No. 1, 1997, pp. 164-166.

[12] Wang, K. C., Separation Patterns of Boundary Layer over an Inclined Body of Revolution, *AIAA Journal*, Vol. 10, No. 8, 1972, pp. 1044-1050.

[13] Zakkay, V., Miyazawa, M., and Wang, C. R., Hypersonic Lee Surface Flow Phenomena over a Space Shuttle, *Journal of Spacecraft and Rockets*, Vol. 12, No. 11, 1975, pp. 667-673.

[14] Murakami, A., Maita, M., Hirabayashi, N., Sekine, H., Sakakibara, S., and Watanabe, Y., Pre-Compression Flow on Fore-Body of Space-Plane at Mach 10, *Proceedings of Fluids Engineering Conference 2000*, Muroran, Japan, 2000, p. 41 (in Japanese) .

[15] Kanda, T., Kato, K., Kodera, M., Kudo, K., and Murakami, A., Effect of Airframe Configuration on Airflow Condition to Engine in Hypersonic Flow, *21st Applied Aerodynamics Conference*, Orlando, FL, USA, AIAA 2003-3420, 2003.

[16] Nomura, S., Hozumi, K., and Kawamoto, I., Experimental Studies on Aerodynamic Characteristics of SSTO Vehicle at Subsonic to Hypersonic Speeds, *Proceedings of the 16th International Symposium on Space Technology and S*cience, Sapporo, Japan, 1988, pp. 1547-1554.

[17] Kubota, S., Masuya, G., and Tani, K., Aerodynamic Performances of Combined Cycle Inlet, *Proceedings of 24th Congress of the International Council of the Aeronautical Sciences*, Yokohama, Japan, ICAS 2004-6.6.1, 2004.

[18] Sakata, K., Yanagi, R., Shindo, S., Minoda, M., and Nouse, H., Conceptual Study on Air-Breathing Propulsion for Space Plane, *Proceedings of 16th International Symposium on Space Technology and Science*, Sapporo, Japan, 1988, pp. 107-112.

[19] Akihisa, D., Kanda, T., Tani, K., Kudo, K., and Masuya, G., Effect of Integration of Scramjet into Airframe on Engine Performance and Payload, *Journal of Propulsion and Power*, Vol. 18, No. 5, 2002, pp. 1026-1032.